PERFORMANCE ANALYSIS OF MULTIWAVELETS CONSTRUCTED USING B-SPLINE REFINABLE SUPER FUNCTIONS

Huseyin Ozkaramanli and Burcin Ozmen

Department of Electrical and Electronic Engineering
Eastern Mediterranean University
Gazimağusa, Cyprus
(burcin.ozmen@emu.edu.tr; huseyin.ozkaramanli@emu.edu.tr)

ABSTRACT

Image compression performance of new multiwavelets constructed using B-spline super functions is compared with existing multiwavelets. First orthogonal, approximation order preserving pre-filters are designed and then an extensive comparative performance analysis in image compression is carried out. Our results confirm the usefulness of the super function design criteria in image compression. The new multiwavelets show excellent performance, which is better than most of the well known multi-wavelets and at least as good as the 9/7 biorthogonal wavelet.

1. INTRODUCTION

Ever since their discovery, multi-wavelets have been the focus of a lot of research in signal processing and pure mathematics [1]-[5]. The interest in multiwavelets is mainly due to the fact that, unlike scalar wavelets, they can simultaneously possess orthogonality and symmetry. Furthermore, it is possible to combine high order of approximation and short support.

Approximation order is an important feature for wavelet applications. Its characterization forms the basis for constructing new multiwavelets. Super function theory is an elegant way of characterizing approximation order [6]. In this work we briefly review the formulation of a simple criterion which ensures that a given refinable super function with desired approximation order (e.g. a basic spline) lies in the linear span of integer translates of the multiscaling functions. This ensures that the multiscaling functions inherit the approximation order of the super function. Using the derived condition, we then give the construction of a symmetric and a non-symmetric multi-wavelet where the B-spline super function of order two lies in the linear span of integer translates of their multiscaling functions. Thus they both have approximation order three [7]. Quasi optimum orthogonal approximation order preserving pre-filters for both are designed using the method described in [8]. The pre-filters are designed so that the pre-filter - multifilter combination produce the lowest mean square error in one dimensional sinusoidal signal representation with a specific number of coefficients in the approximation. The performances of the new multiwavelets are compared with existing multiwavelets with their best pre-filters. Our results indicate that the new multiwavelets outperform almost all other multiwavelet transforms for almost all images considered.

2. MULTIWAVELETS VIA B-SPLINE SUPER FUNCTIONS

In this section, we review the derivation of a simple condition which ensures that a given refinable super function lies in the linear span of integer translates of the multiscaling functions. The condition is formulated as a generalized eigenvalue equation which provides a method for constructing the r scaling functions from a known refinable super function [7]. Requiring the compactly supported and refinable super function $f(t)$ to lie in the finite linear span of integer translates of multiscaling functions $\boldsymbol{\Phi} = \left(\phi_0 \;\; \phi_1 \;\; . \; . \; . \;\; \phi_{r-1}\right)^T$, we obtain

$$f(t) = \sum_{n} \sum_{k} a_k^n \phi_n(t-k) \tag{1}$$

where a_k^n are finite sequences in the linear combination. The refinability of the super function implies that it satisfies the dilation equation with a scalar scaling filter h_ℓ

$$f(t) = \sum_{\ell} h_\ell f(2t-\ell) \tag{2}$$

Similarly, the multiscaling functions satisfy the vector dilation equation

$$\boldsymbol{\Phi}(t) = \sum_{k} \boldsymbol{c}_k \boldsymbol{\Phi}(2t-k) \tag{3}$$

where $\boldsymbol{c}_k$ is a finite sequence of real 2 x 2 matrices.

Combining (1) and (2) gives

$$\sum_{n} \sum_{k} a_k^n \phi_n(t-k) = \sum_{\ell} h_\ell \left\{ \sum_{n} \sum_{k} a_k^n \cdot \phi_n(2t-k-\ell) \right\} \tag{4}$$

	k	$\boldsymbol{c}_k$	$\boldsymbol{d}_k$
MWs_p3	0	0.01319014879908 -0.00103170465482 0.01612422454349 -0.00126120165666	-0.10107171197121 0.00790560874635 -0.00042549290059 0.00003328112615
	1	0.00991343500792 -0.12674139081667 0.01211862386845 -0.15493431314630	-0.07596334681497 0.97117701570962 -0.00031979140497 0.00408847260362
	2	0.68400319737956 -0.12570968616184 0.68940144308205 0.01767955302216	0.19933707925397 -0.01350431337959 -0.02155673616222 -0.01916908817968
	3	0.68400319737956 0.12570968616184 -0.68940144308205 0.01767955302216	-0.02155673616222 0.01916908817968 0.19933707925397 0.01350431337959
	4	0.00991343500792 0.12674139081667 -0.01211862386845 -0.15493431314630	-0.00031979140497 -0.00408847260360 -0.07596334681497 -0.97117701570962
	5	0.01319014879908 0.00103170465482 -0.01612422454349 -0.00126120165666	-0.00042549290058 -0.00003328112615 -0.10107171197121 -0.00790560874635
GHM_p3	0	-0.00000000000000 -0.21427906746710 -0.00000000000000 -0.05080667958406	0.00000000000000 -0.42387365634026 -0.00000000000000 0.02883143939738
	1	0.76788573748733 -0.59294475226534 0.14015502335727 0.03618641554837	-0.61227829542638 -0.65942860917543 -0.07953424815881 -0.02053482840116
	2	0.11336885008659 -0.00000000000000 -0.85608441929855 0.43336471404075	-0.10295786425264 -0.00000000000000 0.48580513932648 0.76367405268378
	3	0.00000000000000 0.00000000000000 -0.04809874213420 -0.22715838046850	0.00000000000000 0.00000000000000 -0.08475946505225 -0.40029784473211
	4	0.00000000000000 0.00000000000000 -0.04319568165697 0.00000000000000	0.00000000000000 0.00000000000000 -0.07611930598095 0.00000000000000

Table 1: Matrix filters coefficients of multiwavelets.

Expanding the left hand side of (4) using the matrix dilation equation and matching terms of the same scale and shift on both sides results in

$$\mathbf{x}\boldsymbol{H}_{\mathrm{f}} = \mathbf{x}\boldsymbol{B}_{\mathrm{f}} \qquad (5)$$

where $\mathbf{x} = [\boldsymbol{x}_0\ \boldsymbol{x}_1\ \ldots\ \boldsymbol{x}_{K-1}]$ with $\boldsymbol{x}_k = [a_k^0\ a_k^1\ \ldots\ a_k^1]$, $\boldsymbol{H}_f$ and $\boldsymbol{B}_f$ are finite portions of the infinite matrices $\boldsymbol{H}$ and $\boldsymbol{B}$ respectively,

$$\boldsymbol{H} = \begin{pmatrix} \cdot & \cdot & & & & & & \\ & & \boldsymbol{c}_0 & \boldsymbol{c}_1 & \cdot & \cdot & \boldsymbol{c}_{N-1} & \\ & & & \boldsymbol{c}_0 & \boldsymbol{c}_1 & \cdot & \cdot & \boldsymbol{c}_{N-1} \\ & & & & & & \cdot & \cdot \end{pmatrix},$$
$$\boldsymbol{B} = \begin{pmatrix} \cdot & \cdot & \cdot & & & & & \\ & & h_0\boldsymbol{I} & h_1\boldsymbol{I} & \cdot & \cdot & h_{L-1}\boldsymbol{I} & \\ & & & h_0\boldsymbol{I} & h_1\boldsymbol{I} & \cdot & \cdot & h_{L-1}\boldsymbol{I} \\ & & & & & & \cdot & \cdot \end{pmatrix} \qquad (6)$$

In (6), $\boldsymbol{I}$ is the 2 x 2 identity matrix and N and L denote the supports of the multiscaling function and refinable super function respectively. Equation (5) forms the starting point for the construction of multiscaling functions with approximation order. It has non-trivial solutions if the matrix $(\boldsymbol{H}_f - \boldsymbol{B}_f)$ is not of full rank. Any vector $\mathbf{x}$ in the left null space of $(\boldsymbol{H}_f - \boldsymbol{B}_f)$ can be used in the linear combination (1) to produce the super function $f(t)$.

Once the matrix filter coefficients of the multiscaling function are evaluated, the multi-wavelets, $\Psi = (\psi_0\ \psi_1\ \ .\ .\ .\ \psi_{r-1})^T$, which satisfy the matrix dilation equation with matrix coefficients $\boldsymbol{d}_k$

$$\Psi(t) = \sum_k \boldsymbol{d}_k \boldsymbol{\Phi}(2t-k) \qquad (7)$$

can be constructed to be orthogonal to the multiscaling functions [2].

In [7], based on the super function formulation, two new multiwavelets with approximation order three were constructed. The first construction (GHM_p3) was defined by five 2x2 matrix filter coefficients and was non-symmetric. The second construction (MWs_p3) was a symmetric multiwavelet system defined by six 2x2 matrix filter coefficients. The coefficients $\boldsymbol{c}_k$ of multiscaling functions and $\boldsymbol{d}_k$ of multiwavelets are listed in Table 1. Multiscaling and multiwavelet functions of the second construction (MWs_p3) is shown in Fig. 1.

In application using multiwavelets, it is necessary to associate a given discrete signal with a function in the scaling function space V_0 [9]. This association is equivalent to including a pre-filter and a post-filter for the filter bank determined by the underlying multiwavelets. Using the method described in [8] a set of quasi-optimum orthogonal approximation order preserving pre-filters are designed for the new multiwavelets. The pre-filters are optimum in the sense that they are designed using an exhaustive search algorithm to give minimum peak signal to noise ratio (PSNR) when approximating one dimensional sinusoidal waveforms with a specified number of coefficients kept in the reconstruction. In Table 2 the coefficients of quasi-optimum pre-filters for both multiwavelets are given.

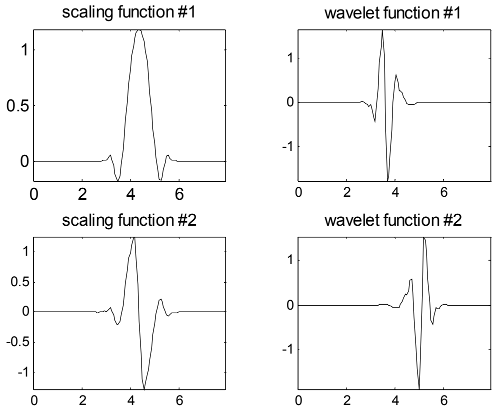

Fig. 1: Multiscaling and multiwavelet functions of MWs_p3.

		Quasi-optimal pre-filters
GHM_p3	q(1)	0.05469185477583 0.98776815866677 0.00807282833252 0.14580018925901
	q(0)	0.14580018925901 -0.00807282833252 -0.98776815866677 0.05469185477583
MWs_p3	q(1)	0.00140124612474 0.00242930883535 0.00501192331030 0.00868905852072
	q(0)	0.71439459358253 0.69966554904089 0.69966554904089 -0.71439459358253
	q(-1)	-0.00868905852072 0.00501192331030 0.00242930883535 -0.00140124612474

Table 2: Orthogonal pre-filters for MWs_p3 and GHM_p3 multiwavelets.

3. APPLICATION TO IMAGE COMPRRESSION

In this section the performance of the new multiwavelets are compared with GHM [1], CL [5] and SA4 [4] multiwavelets. The best known pre-filters [4], [8] for these multiwavelets are employed in the comparison. Five iterations of the cascade algorithm are implemented. The same number of coefficients is retained by killing coefficients below a threshold defined by the compression ratio (CR) for all multiwavelet transforms and finally the cascade algorithm is inverted to reconstruct the original image. For symmetric multiwavelets, the boundaries are handled by symmetrically extending the data and for the non-symmetric GHM_p3 multiwavelet a periodic wrap of the data is applied. No coding is employed since we are interested in the energy compaction properties if newly constructed multiwavelets. The results of our simulations for six standard images are given in Table 3. We indicate with boldface numbers the wavelet that performs best in the peak signal to noise ratio sense (PSNR). It is observed that MWs_p3 outperforms almost all the other multi-wavelets for a big majority of images at almost all compression ratios considered. The situation is slightly different for Barbara and Baboon images. These images contain significantly higher frequencies. For Barbara image SA4 [4] multiwavelet performs slightly better than MWs_p3 at all compression ratios considered. For Baboon image at low compression ratios SA4 again outperforms MWs_p3; however for compression ratios beyond 24:1 MWs_p3 outperforms SA4. in most cases, the performance obtained by the new multiwavelet MWs_p3 is comparable to the popular Bi 9\7 scalar biorthogonal wavelet. For the Lena image Bi 9\7 outperforms slightly the MWs_p3 multiwavelet. Also, for the Yogi image at low compression ratios Bi 9\7 is about 2 dB better than best multiwavelet studied in this work. Figure 2 displays the reconstructed Lena images with MWs_p3, GHM_p3, CL [5] and SA4 [4] multiwavelets together with Bi 9\7 wavelet at compression ratio 128:1. The best known pre-filters [4], [8] for SA4 [4] and CL [5] multiwavelets are also employed in the comparison.

4. CONCLUSION

Image compression performance of multiwavelets constructed to have a B-spline super function in the linear span of the integer translates of their multiscaling functions is evaluated. The usefulness of this property is demonstrated. It is shown that with the appropriate design of pre-filters, the new multiwavelets give excellent performance outperforming almost all the other multi-wavelets both visually and in the peak signal to noise sense. The performance are comparable to those of the popular Bi 9\7 biorthogonal scalar wavelet in most cases.

5. REFERENCES

[1] J.S. Geronimo, D.P. Hardin and P.R. Massopust, “Fractal Functions and wavelet expansions based on several scaling functions”, *J. Approx. Theory*, vol. 78, pp.373-401, 1994.

[2] G. Strang, V. Strela, “Short Wavelets and Matrix Dilation Equations”, *IEEE Trans. on Signal Processing*, vol. 43, no.1, pp108-115, 1995.

[3] V. Strela, P.N. Heller, G. Strang, P. Topiwala and C. Heil, “The application of multi-wavelet filter banks to signal and image processing”, *IEEE Trans. on Image Processing*, 8(4), pp. 548-563, 1999.

[4] L. Shen, H.H. Tan and J.Y. Tham, “Symmetric-Anti-symmetric Orthonormal Multi-wavelets and related scalar wavelets”, *Applied Comput. Harmon. Anal.*, 8, pp. 258-279, 2000.

[5] C.K. Chui, and J.A. Lian, “Study of Orthonormal Multi-wavelets”, *J. Applied Numerical Math*, vol.20, no.3, pp. 273-298, 1996.

[6] C. DeBoor, R.A. DeVore and A. Ron, “Approximation orders of FSI spaces in L2(Rd)”, *Constr. Approx.*, vol. 14, pp. 411-427, 1998.

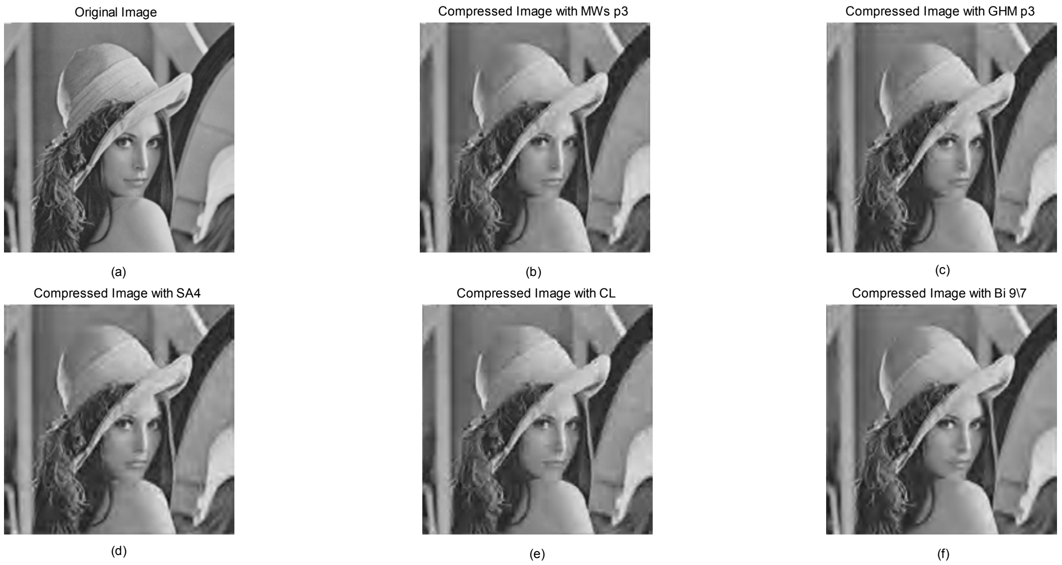

Fig. 2: Original image is shown in (a).Reconstructed Lena image with MWs_p3, GHM_p3, SA4, CL multiwavelets and Bi 9\7 wavelet are shown in (b), (c), (d), (e), and (f), respectively.

	CR	PSNR (dB)					
		MW _p3	GHM _p3	GHM	CL	SA4	Bi9\7
Goldhill	8:1	**35.68**	35.05	35.09	35.23	35.55	35.47
	16:1	**32.74**	32.10	32.08	32.27	32.56	32.47
	32:1	**30.43**	29.83	29.78	29.98	30.23	30.12
	64:1	**28.49**	27.95	27.91	28.08	28.31	28.20
	128:1	**26.79**	26.37	26.30	26.45	26.64	26.59
Lena	8:1	38.94	38.91	38.56	38.70	38.94	**39.15**
	16:1	35.72	35.54	35.16	35.27	35.67	**35.93**
	32:1	32.64	32.36	31.95	32.02	32.50	**32.76**
	64:1	29.82	29.55	29.02	29.13	29.59	**29.86**
	128:1	**27.35**	27.12	26.56	26.69	27.02	27.32
Barbara	8:1	27.95	27.85	27.76	27.69	**28.19**	27.82
	16:1	25.80	25.66	25.54	25.50	**26.04**	25.66
	32:1	24.02	23.87	23.77	23.76	**24.27**	23.79
	64:1	22.58	22.44	22.35	22.39	**22.79**	22.34
	128:1	21.50	21.36	21.27	21.34	**21.62**	21.33
Boats	8:1	**38.92**	37.76	37.81	38.21	38.58	38.60
	16:1	**34.65**	33.40	33.38	33.87	34.24	34.19
	32:1	**31.22**	30.17	30.09	30.48	30.90	30.71
	64:1	**28.48**	27.62	27.59	27.86	28.22	27.98
	128:1	**26.23**	25.63	25.58	25.85	25.95	25.88
Yogi	8:1	37.46	37.05	35.61	39.33	36.33	**39.35**
	16:1	30.03	29.45	28.18	29.84	29.20	**30.10**
	32:1	**25.58**	25.15	24.30	25.02	24.96	25.21
	64:1	**22.62**	22.29	21.86	22.10	22.20	22.40
	128:1	**20.60**	20.26	20.06	20.14	20.25	20.47
Baboon	8:1	28.50	28.47	28.32	28.26	**28.61**	28.57
	16:1	25.85	25.76	25.62	25.62	**25.90**	25.82
	32:1	**24.09**	23.96	23.83	23.86	24.08	24.01
	64:1	**22.85**	22.75	22.62	22.66	22.83	22.77
	128:1	**21.98**	21.89	21.79	21.82	21.95	21.90

Table 3: Still image compression performance comparisons.

[7] D.P. Hardin, and D.W. Roach, “Multi-wavelet prefilters I: Orthogonal prefilters preserving approximation order $p \leq 2$”, *IEEE Trans. on Circuits and Systems II*, vol. 45, no. 8, pp. 1106-1112, 1998.

[8] X.-G. Xia, J.S. Geronimo, D.P. Hardin, and B.W. Suter, “Design of pre-filter for discrete multiwavelet transform”, IEEE Signal Processing, vol. 44, pp. 25-35, 1996.